Polym. Bull. (2010) 64:445–457
DOI 10.1007/s00289-009-0156-6

ORIGINAL PAPER

Effect of dealcoholation of support in $MgCl_2$-supported Ziegler–Natta catalysts on catalyst activity and polypropylene powder morphology

Ebrahim Jalali Dil · Saeed Pourmahdian · Mohammad Vatankhah · Faramarz Afshar Taromi

Received: 19 March 2009 / Revised: 13 August 2009 / Accepted: 6 September 2009 /

Abstract Spherical support was produced using melt quenching method. Scanning electron microscopy (SEM) images showed that support particles have a rough surface morphology with small pore sizes. The size of primary particles determined to be about 50 nm. Produced particles were dealcoholated using hot nitrogen flow. In this study, the dealcoholation apparatus was similar to a fluidized bed reactor. It consists of three main zones: heating zone, bed zone, and expansion zone. This apparatus is capable to dealcoholate and elutriate support particles at the same time. Results showed a significant increase in specific pore volume and surface area of support particles during the dealcoholation. According to the obtained results, two mechanisms were proposed to explain effect of the dealcoholation on the morphology of support particles. Three dealcoholated samples of different alcohol contents were used in the catalyst preparation. Results showed that by decrease in alcohol content of support particles, specific surface area, and pore volume of catalysts increased. Moreover, titanium content of final catalysts increased slightly. Polymerization of propylene was carried out using obtained catalysts in slurry phase. An increase in catalyst activity and enhancement of polypropylene powder morphology were observed as the alcohol content of support particles decreased.

Keywords Ziegler–Natta catalyst · Dealcoholation · Spherical support · Polypropylene · Slurry polymerization

Introduction

Today spherical-supported Ziegler–Natta catalysts are widely used as polymerization catalysts in propylene polymerization. The most important advantage of this

---

E. Jalali Dil · S. Pourmahdian (✉) · M. Vatankhah · F. Afshar Taromi
Polymer Engineering Department, Amirkabir University of Technology, 15914 Tehran, Iran
e-mail: Pourmahd@aut.ac.ir

type of catalyst is the possibility of controlling morphology of polymer from supported catalyst that is a result of replication phenomena, duplication of the catalyst shape in the polymer particle. The potential advantages of controlled morphology particles, such as high bulk density, narrow particle size distribution, elimination of excess fines, and higher flowability of polymer powder are broadly accepted [1, 2]. For these reasons, catalysts with controlled spherical morphology were developed allowing the full control of particle size and porosity of final polymer [2]. In order to achieve controlled morphology particles, some requirements were presented, such as sufficiently high concentration of active centers, homogeneous distribution of active sites, ready access of monomer to every point within the particle, sufficient support fragility to permit subdivision of particle into primary particles during polymerization, and sufficient integrity in the polymer to retain all parts of a single catalyst particle in a single polymer particle [1]. According to above requirements, the most important parameter that has a dominant role in controlling particle morphology is porosity of support particles. Melt quenching of molten $MgCl_2 \cdot n$EtOH is a common method to produce spherical support for polymerization catalysts [3–12]. Obtained support from this method has low surface area and porosity. If obtained support directly reacts with $TiCl_4$, final catalysts with fragile structure and low specific surface area will be produced. Also, some by-products such as trichloro titanium ethoxide are produced due to exothermic reaction of $TiCl_4$ and ethanol [7]. Therefore, obtained catalyst has low activity and produces fine polymer particles. In order to increase specific surface area and modifying porosity of support, an intermediate dealcoholation step has been used since 1980. There are three methods to dealcoholate support particles: (a) dealcoholation under hot nitrogen flow [7, 8, 10, 12, 13, 14, 16] (b) dealcoholation under vacuum with controlled heat, and (c) reaction of support particles with triethylaluminum [7]. Among these methods, dealcoholation under hot nitrogen flow is widely used by scientists and industries due to its better control over final particle morphology and higher efficiency. The dealcoholation process has such an important role in catalyst preparation that many articles and patents have been published on this issue. Even in last years, scientists considered the dealcoholation as a controversial issue [11, 12, 15]. Almost all of previous studies have mentioned that the dealcoholation resulted decrease in catalyst activity and polypropylene isotacticity [7, 8, 10, 12, 13, 16]. Even if improvement of polymer morphology is considered as an advantage of using the dealcoholation, we cannot ignore significant decrease in catalyst activity and polypropylene isotacticity that have been reported by the previous authors. Dramatic effect of dealcholation on catalyst activity can be attributed to decease in surface area and titanium content of final catalyst. According to previous studies [7, 16, 18], decrease in catalyst surface area can be attributed to collapse of support structure during catalyst preparation which is a result of poor support structure. Moreover, in spite of the important role of the dealcoholation on support morphology, we could not find any previous study that studied the effects of the dealcoholation on support morphology. Therefore, in this study, attempts have been made to find a dealcoholation procedure that not only improves powder morphology but also increases catalyst activity. Also, effect of dealcoholation on support morphology was studied, and two mechanisms were proposed to be engaged in evolution of support morphology during the dealcoholation. This provides an insight to understand the effects of the dealcoholation on final catalyst characteristics.

Experimental

Materials

Anhydrous magnesium chloride, paraffin oil, ethanol (>99.5%), titanium tetrachloride (>99.8%), diisobutyl phthalate, and cyclohexyl dimethoxy methylsilane were purchased from Sigma-Aldrich, and were used as received. Triethylaluminum solution in hexane (1,200 mmol/L) was taken from Bandar Imam Petrochemical Complex and was used as received. Hexane (>98.5%) and heptane (>98.9%) were taken from Bandar Imam Petrochemical Complex and stored over 4 Å molecular sieves. Propylene (>99.9%) and hydrogen were supplied by Research Institute of Petroleum Industries (RIPI). Commercial catalyst, $MgCl_2/ID/TiCl_4$, was supplied by Navid Zar Chimie Co.

Catalyst preparation

According to the method described in Ref. [9], support preparation was carried out. Prepared support was named as SD28. The dealcoholation apparatus was similar to a fluidized bed reactor and consist of three main zones: heating zone, bed zone, and expansion zone (Fig. 1). Nitrogen entered to the heating zone at ambient temperature, and was heated to desired temperature. A PID temperature controller controlled the temperature of nitrogen at heating zone exit (±0.1 °C).

Nitrogen flow rate was controlled to be 60 mL/s. When temperature of nitrogen at the exit of heating zone became constant, 10 g of support was added to the bed zone. Figure 1 shows time–temperature history and variation of alcohol content of support during the dealcoholation. Two samples were prepared, and were named as SD23 and SD18. The method that was used to prepare final catalyst was similar to the method presented by Ferraris et al. [9]. Ten grams of support were added to a reactor contained $TiCl_4$ (Ti/Mg molar ratio $= 40$) at -10 °C. Reactor temperature was increased to 90 °C at heating rate of 0.55 °C/min. When reactor temperature reached 50 °C, diisobutyl phthalate was added (Mg/diisobutyl phthalate molar ratio $= 8$) as internal donor. The mixture was remained at 90 °C for 90 min. Then, the reactor was discharged, and fresh titanium tetrachloride was added. Reactor temperature was increased to 120 °C and remained for 1 h. Finally, the reactor was cooled down to the room temperature. Final catalysts were washed with hexane. Washing of catalyst with hexane continued until the amount of titanium in filtrate became less than 1,000 ppm. According to Ref. [19], this criterion was chosen as an indication of absence of impunities in final catalyst. In order to determine amount of titanium in filtrate, UV absorption test was employed. The resultant catalysts were named CSD28, CSD23, and CSD18, which were prepared from SD28, SD23, and SD18, respectively. Prepolymerization was carried out under non-isothermal condition. Slurry polymerization of

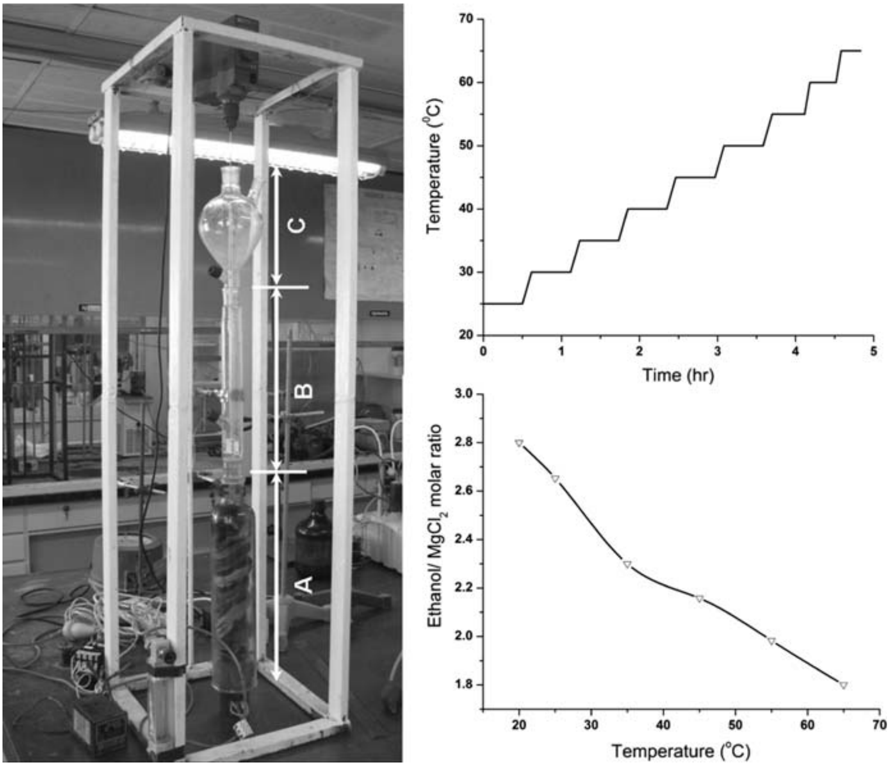

Fig. 1 *Right*: Time–temperature history and variation of alcohol content of support during the dealcoholation. *Left*: The dealcoholation apparatus. (*A*) Heating zone, (*B*) bed zone, and (*C*) expansion zone

Table 1 Polymerization conditions

Temperature (°C)	Reactor pressure (atm)	Hydrogen pressure (kg/cm^2)	Cocatalyst concentration in reactor (mmol/L)	Cocatalyst to external donor molar ratio
70	5	0.5	1.5	10

propylene was carried out. Table 1 shows the polymerization conditions. An average value over three consecutive polymerization experiments was reported as catalyst activity.

Analytical techniques

In order to determine EtOH/$MgCl_2$ molar ratio, five standard solutions with 4, 10, 16, and 25 volume percentage of ethanol in water were prepared. Each standard solution contained 10 volume percentage of *n*-propanol. One gram of support was dissolved in 10 mL of dime neutralized water. Sufficient *n*-propanol was added to attain the same concentration of that was created in standard solutions. Then, this solution was diluted to 25 mL by addition of dime neutralized water. Gas chromatography was performed (Agilent 6890N) using Thermal conductivity detector (TCD). Oven temperature, detector temperature, and injection temperature were 110, 150, and 150 °C, respectively. After determining peak areas in chromatograms of standard solutions, ratio of area of ethanol peak to area of *n*-propanol peak was calculated, and a plot of relative peak area ratio versus volume percentage of ethanol was prepared. Solution of support in dime neutralized water was injected, and volume percentage of ethanol in the sample (prior to dilution) was determined using prepared plot. Finally, EtOH/$MgCl_2$ molar ratio was calculated using obtained results. UV absorption test (HACH, DR/4000U, $\lambda = 420$ nm) was used to determine titanium content of catalyst samples. Weight percentage of titanium in catalyst samples was calculated as follows:

$$\text{Weight Percentage of Ti} = (\text{Absorption} \times 0.47)/0.728 \qquad (1)$$

Particle size distribution of support and catalyst were determined by low-pressure mercury porosimetry (Thermo Finnigan, Pascal 140) due to non-destructive nature of this test method. Average particle size was determined as particle diameter at 50% of cumulative volume. Micro-pore size distribution, specific pore volume and specific surface area of support and catalyst were measured using nitrogen physisorption (Thermo Finnegan, Sorptomatic 1990) at liquid nitrogen temperature. Average pore radius was determined as pore radius at 50% of cumulative pore volume. Scanning electron microscopy (Philips, XL30) was used to study morphology of support, catalyst, and polypropylene particles. Particle size distribution of polypropylene samples was determined using a shaker equipped with different sieves had mesh sizes from 40 to 4,000 μm. Each test lasted for 10 min at shaking amplitude of 1.3 mm. According to ASTM D1895 type A, bulk density of polypropylene powder was measured.

Results and discussion

Ethanol to magnesium chloride molar ratio of sample SD28 determined to be 2.8. Figure 2 shows particle size distribution of this sample. Average particles size was determined to be 48 μm. Also, SPAN value (measure of the width of the volume distribution relative to the median diameter [7]) was determined to be 1.29 which is a characteristic of narrow particle size distribution. Specific surface area and specific pore volume of SD28 are listed in Table 2. Also, micro-pore size distribution of this sample is shown in Fig. 3. These results determine highly packed structure with small pore sizes. Specific surface area and specific pore volume of dealcoholated samples, SD23 and SD18, are listed in Table 2. Results showed that pore size and specific pore volume were increased during the dealcoholation. Figure 3 shows changes in micro-pore distribution of support during the dealcoholation.

Scanning electron microscopy (SEM) images were employed to interpret these results. As can be seen, Fig. 4, by decreasing alcohol content of support particles, support morphology shifted to highly porous structure with large pore size. The

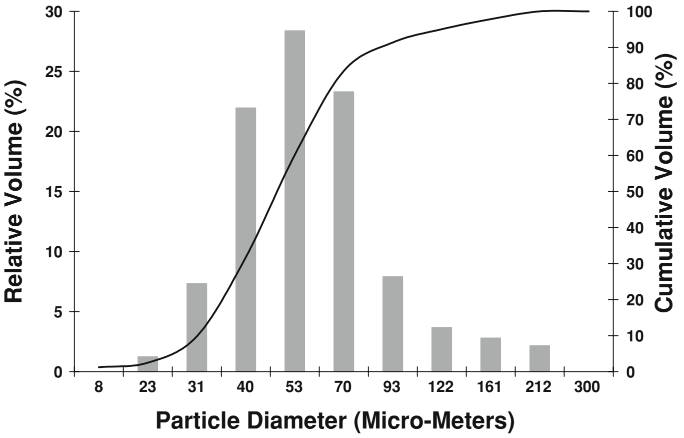

Fig. 2 Particle size distribution of sample SD28

Table 2 Specific surface area and specific pore volume of support samples

Sample name	Ethanol/$MgCl_2$ molar ratio	Specific surface area (m^2/g)	Specific pore volume (cm^3/g)
SD28	2.8	2.31	0.434
SD23	2.3	4.16	0.531
SD18	1.8	11.38	0.623

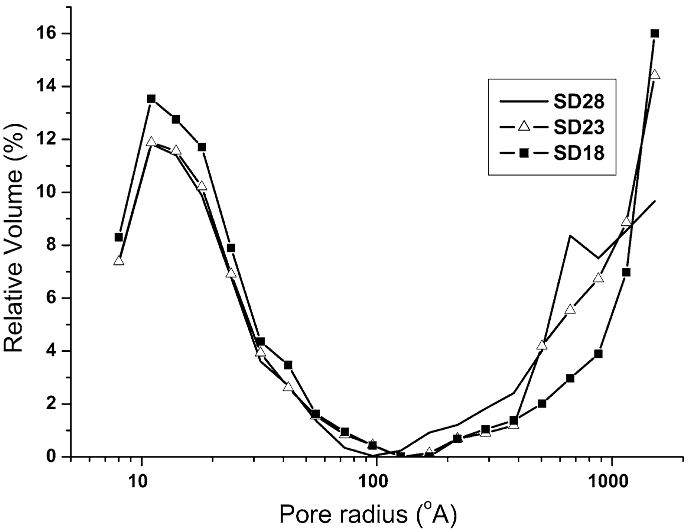

Fig. 3 Micro-pore size distribution of support samples

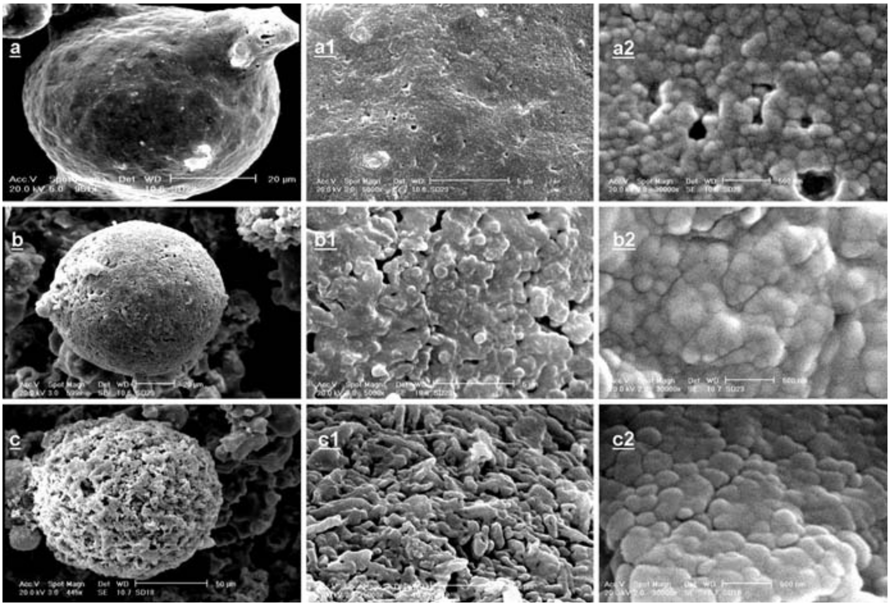

Fig. 4 SEM images of support samples: (**a**) SD28, (**b**) SD23, and (**c**) SD18. **a1**, **b1**, and **c1** (*center column*; 5,000×) and **a2**, **b2**, and **c2** (*right column*; 30,000×) show surface morphology of support samples SD28, SD23, and SD18, respectively

morphology of sample SD23 is similar to the morphology that Guan et al. [13] reported for a dealcoholated support. According to the obtained results, evolution of the morphology of support during the dealcoholation can be attributed to two competitive mechanisms: merging of primary particles and cracking due to alcohol transfer from interior surfaces. During the dealcoholation and by increasing nitrogen temperature, primary particles merged together. This phenomenon happened due to high alcohol content of primary particles that lowered their melting point. Merging of primary particles caused elimination of micro-pores and, consequently, reduced alcohol transfer to particles' surface. By further increase in nitrogen temperature, the stress exposed to interior surfaces of support by vaporized ethanol caused cracking of these surfaces, which enhanced alcohol transfer to particles' surface. These cracks ranged from small cracks to large ones. At high alcohol content of support particles, micro-cracks were healed due to second merging of primary particles. Consequently, at this stage, only large cracks could remain (Fig. 4b1, b2). At higher temperature, which means lower alcohol content, crack healing mechanism weakened. The main reasons are increase in melting point of primary particles due to decrease in their alcohol content and increase in the primary particles size. Therefore, the primary particles only fused superficially (Fig. 4c1, c2). This is the main reason of increasing population of micro-pore (<100 µm) at this stage (Fig. 3).

Sozzani et al. [8] and Xu et al. [12] used a fluidized bed reactor to carry out the dealcoholation. The difference between their method and the presented method is in time–temperature history. Also, they did not focus on the dealcoholation and the origin of its effects on the catalyst characteristics. Moreover, they did not report some operation conditions such as gas flow rate, which has a significant effect on the dealcoholation and dealcoholated support morphology.

Jamjah et al. [11] presented a figure of a dealcoholated support particle that shows morphology similar to SD28, but he reported higher specific surface area. Also, Forte and Coutinho [7] carried out the dealcoholation, but he did not study variation of surface morphology and micro-pore size distribution during the dealcoholation. Moore [1] presented an image of a dealcoholated support particle that has rough surface morphology with large pore sizes. The difference in the morphology of dealcoholated support particles can be attributed to the difference in the time–temperature history. In fact, final support morphology is completely dependent on time–temperature history. This parameter determined which mechanism becomes dominant in the dealcoholation. Therefore, the final morphology can vary from a highly porous structure to highly packed structure with large pore sizes. Final catalysts were prepared by reacting support samples with $TiCl_4$. Titanium contents of catalyst samples are listed in Table 3.

Results showed that the titanium content of final catalysts increased by decreasing alcohol content of support. Forte and Coutinho [7] reported an increase in titanium content of final catalyst by decreasing alcohol content. This is due to increase in surface area of support during the dealcoholation that provided new surfaces for reaction of $TiCl_4$. Specific surface area and specific pore volume of catalyst samples are listed in Table 4. As can be seen, specific surface area and specific pore volume of final catalyst increased as the alcohol content of support decreased.

Evangelisti et al. [15] and Sacchetti et al. [16] reported that by decrease in alcohol content of support, specific surface area of support increased, but the specific surface area of final catalyst decreased. This is due to collapse of support structure during catalyst preparation which is a result of poor support structure. In

Table 3 Titanium content of catalyst samples

Sample name	Weight percentage of Ti
CSD28	3.09
CSD23	3.66
CSD18	4.32

Table 4 Specific surface area, specific pore volume and average micro-pore size of catalyst samples

Sample name	Ethanol to magnesium chloride molar ratio of support	Specific surface area [BET method (m^2/g)]	Specific pore volume; BJH method, C = 0.75 (cm^3/g)	Average micro-pore sizes (Å)
CSD28	2.8	82.7	0.359	18.9
CSD23	2.3	117.6	0.437	21.0
CSD18	1.8	201.2	0.588	21.3

the method presented here, the time–temperature history was controlled to avoid this phenomenon by maintaining the strength of support structure. In fact, if the dealcoholation carries out with high temperature elevation rate, final support with fragile structure will be produced. This is due to domination of cracking mechanism. On the other hand, if the dealcoholation carries out at low temperature elevation rate, final support particle with packed structure and large pore sizes will be obtained. Figure 5 shows SEM images of catalyst samples. Also SEM image of a commercial catalyst, $MgCl_2/ID/TiCl_4$ is shown for comparison. As can be seen, the morphology of CSD18 is very similar to that of commercial catalyst. Table 5 shows catalysts activity in slurry polymerization of propylene.

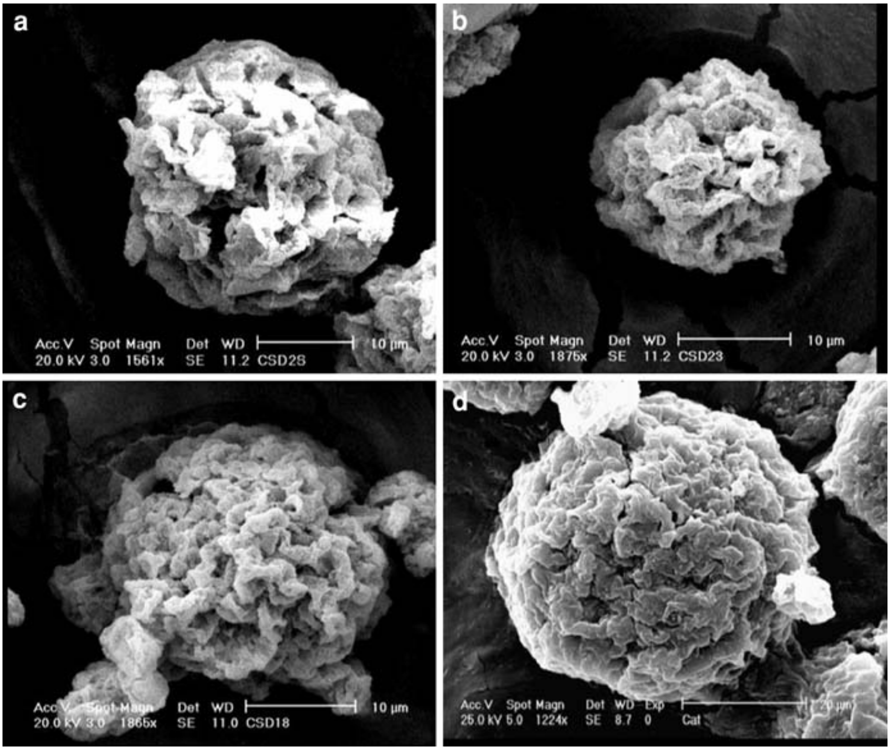

Fig. 5 SEM image of (**a**) CSD28, (**b**) CSD23, (**c**) CSD18, (**d**) commercial catalyst

Table 5 Catalyst activity and bulk density of produced polypropylene powders

Sample name	Activity $\left(\frac{\text{kg}}{\text{mol}}\frac{\text{Polypropylene}}{\text{Ti}\times\text{MPa}\times\text{h}}\right)$	Bulk density of produced polypropylene powder (g/cm^3)
CSD28	8,282	0.377
CSD23	8,774	0.409
CSD18	10,243	0.428

These results are in contrary with the results that Sacchetti et al. [16] and Moore [1] reported. In fact, the activity of catalyst should decrease at low alcohol content (EtOH/$MgCl_2$ molar ratio lowers than 1). This is due to decrease in catalyst surface area that is a result of poor support structure. Nevertheless, at moderate values (EtOH/$MgCl_2$ molar ratio between 1.5 and 2), and by applying appropriate time–temperature history in the dealcoholation step, catalysts with higher activity can be obtained from support particles with lower alcohol content. Increase in activity of catalyst by decreasing alcohol content can be attributed to increase in titanium content and porosity of final catalyst which enhanced monomer diffusion through growing particles and heat transfer from active centers. Consequently, these phenomena led to higher polymerization rate and higher catalyst activity.

Bulk density and particle size distribution of polymer powders were measured to study effects of the dealcoholation on polymer morphology (Fig. 6; Table 5). As can be seen, by decrease in alcohol content of support particles, bulk density of polypropylene powder increased and particle size distribution became narrow.

Moreover, the maximum peak in particle size distribution shifted toward higher values. These results clearly confirm the idea of improving polymer powder morphology by decreasing alcohol content of support particles.

Figure 7 shows morphologies of final polypropylene particles. As can be seen, by decrease in alcohol content, internal morphology changed from eggshell morphology (Fig. 7a1) to a porous structure (Fig. 7c1). Eggshell morphology is a result of highly packed structure of support sample (SD28) that interfered reaction of titanium tetrachloride with interior surfaces of support. Consequently, the concentration of active centers decreased toward the center of catalyst particles. Therefore, propylene polymerized only on the exterior surfaces of catalyst particles. Zheng and Loos [17] reported similar results. The morphology of polypropylene produced by CSD18 can be identified by rough surface with large pore size. The existence of an internal network into polymer particles is a characteristic of this morphology, and

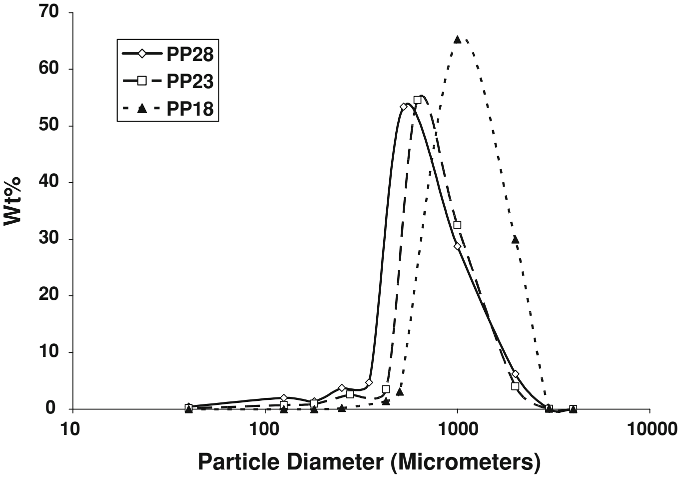

Fig. 6 Particle size distribution of polypropylene powders produced by catalyst samples

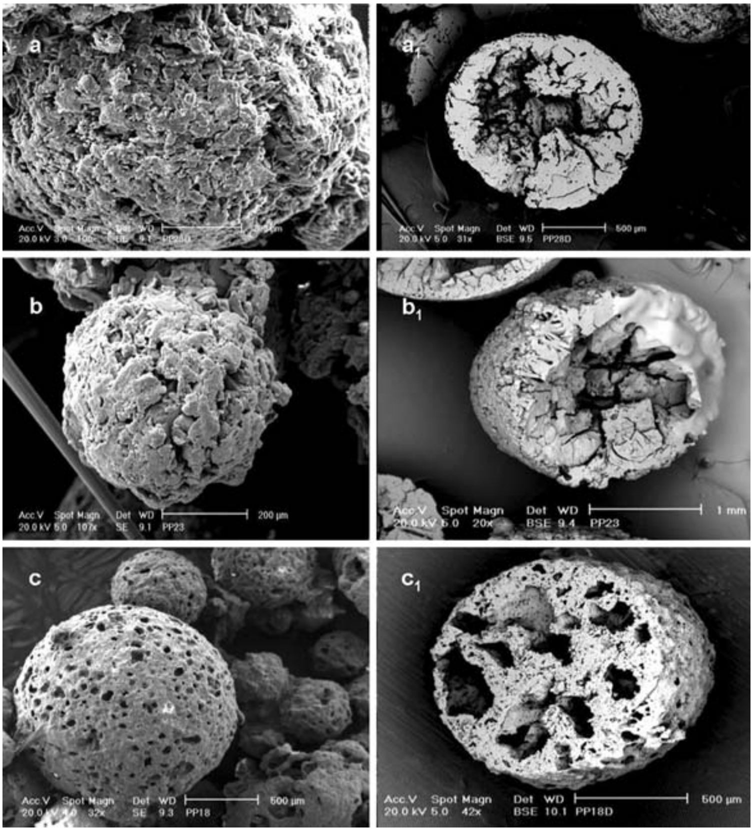

Fig. 7 SEM image of polypropylene produced by: (**a**) CSD28, (**b**) CSD23, (**c**) CSD 18. **a1**, **b1**, and **c1** (*right column*) and **a**, **b**, and **c** (*left column*) show surface morphology and internal morphology of polypropylene particles, respectively

show that CSD18 can be used to produce in situ reactor blends. According to aforementioned time–temperature history that is applied during the dealcoholation has a dominant role in controlling final catalyst and polymer morphology. In this way, by applying appropriate time–temperature history, final catalysts with higher activity and better morphology can be obtained whereas inappropriate time–temperature history results in lower catalyst activity or excess fine particles.

Conclusion

Spherical support was produced using melt quenching method. In order to increase support porosity and modifying its pore size distribution, a dealcoholation step was used. In this step, alcohol content of support particles decreased using hot nitrogen flow. SEM images showed that by decreasing alcohol content, support morphology shifted toward a porous structure. Also, two competitive mechanisms were proposed to be engaged in this process: merging of primary particles and cracking of interior surfaces. Comparison of the present results with the previous studies showed that the final support morphology is completely dependent on time–temperature history. Also, this comparison showed that this parameter not only determines porosity and pore size distribution of final support but also controls the strength of support structure. Three support samples with different alcohol contents were used in catalyst preparation step. Results showed that by decreasing alcohol content of support, catalyst activity increased. This increase can be attributed to ready access of monomer to every point of catalyst particle and enhancement of heat transfer from active centers. Besides, by decreasing alcohol content of support, polymer morphology changed from eggshell morphology to a porous particle with an internal network.

References

1. Moore EP (1998) The rebirth of polypropylene: supported catalysts. Hanser, Munich
2. Galli P, Vecellio G (2001) Technology, driving force behind innovation and growth of polyolefins. Prog Polym Sci 26:1287–1336
3. Monji M, Pourmahdian S, Vatankhah M, Afshar Taromi F (2009) Synthesis of highly improved Ziegler–Natta catalyst. J Appl Polym Sci 112:3663–3668
4. Ling Y, Chen W, Xie L, Liu Y, Zheng G (2008) Preparation of novel microspherical $MgCl_2$-based titanium catalyst for propylene polymerization. J Appl Polym Sci 110:3448–3454
5. Wang L, Yu HJ, Ma ZL, Ye ZY, Jiang S, Feng L, Gu X (2006) Preparation of novel $MgCl_2$-adduct supported spherical Ziegler–Natta catalyst for α-olefin Polymerization. J Appl Polym Sci 99:945–948
6. Ye ZY, Wang L, Feng L, Gu X, Chen H, Zhang P, Pan J, Jiang S, Feng L (2002) Novel spherical Ziegler–Natta catalyst for polymerization and copolymerization. I. Spherical $MgCl_2$ support. J Polym Sci A 40:3112–3119
7. Forte MC, Coutinho MFB (1996) Highly active magnesium chloride supported Ziegler–Natta catalysts with controlled morphology. Eur Polym J 32:223–231
8. Sozzani P, Bracco S, Comotti A, Simonutti R, Camurati I (2003) Stoichiometric compounds of magnesium dichloride with ethanol for the supported Ziegler–Natta catalysis: first recognition and multidimensional MAS NMR Study. J Am Chem Soc 125:12881–12893
9. Ferraris M, Rosati F, Parodi S, Giannetti E, Motroni G, Albizzati E (1983) Catalyst components and catalysts for the polymerization of alpha-olefins. US Patent 4,399,054
10. Govoni G, Ciarrocchi A, Sacchetti M (1993) Crystalline olefin polymers and copolymers in the form of spherical particles at high porosity. US Patent 5,231,119
11. Jamjah R, Zohuri GH, Vaezi J, Ahmadjo S, Nekomanesh M, Pouryari M (2006) Morphological study of spherical $MgCl_2{\cdot}n$EtOH supported $TiCl_4$ Ziegler–Natta catalyst for polymerization of ethylene. J Appl Polym Sci 101:3829–3834
12. Xu R, Liu D, Wang S, Wang N, Mao B (2007) Preparation of spherical $MgCl_2$-supported bis(phenoxyimine) zirconium complex for ethylene polymerization. J Mol Catal A 263:86–92
13. Guan Z, Zheng Y, Jiao S (2002) Spherical $MgCl_2$-supported MAO pre-catalysts: preparation, characterization and activity in ethylene polymerization. J Mol Catal A 188:123–131
14. Evangelisti D, Collina G (2006) Magnesium dichloride-ethanol adducts and catalyst components obtained therefrom. US Patent 7,060,763
15. Evangelisti D, Collina G, Fusco O, Sacchetti M (2006) Magnesium dichloride-ethanol adduct and catalyst components obtained therefrom. US Patent 7,087,688
16. Sacchetti M, Collina G, Ciarrocchi A (1990) Components and catalysts for the polymerization of olefins. Eur Patent 0,395,083
17. Zheng X, Loos J (2006) Morphology evolution in the early stages of olefin polymerization. Macromol Symp 236:249–258

18. Govoni G, Sacchetti M, Ciarrocchi A (1993) Crystalline propylene polymers and copolymers in the form of spherical particles at high porosity. US Patent 5,236,962
19. Chien JCW, Wu JC, Kuo CI (1982) Magnesium chloride supported high mileage catalysts for olefin polymerization. I. Chemical composition and oxidation states of titanium. J Polym Sci A 20: 2019–2032